EPJ manuscript No.
(will be inserted by the editor)

Anisotropic elasticity in confocal studies of colloidal crystals

Michael Schindler and A. C. Maggs

Laboratoire PCT, UMR Gulliver CNRS-ESPCI 7083, 10 rue Vauquelin, 75231 Paris Cedex 05

June 6, 2011

Abstract We consider the theory of fluctuations of a colloidal solid observed in a confocal slice. For a cubic crystal we study the evolution of the projected elastic properties as a function of the anisotropy of the crystal using numerical methods based on the fast Fourier transform. In certain situations of high symmetry we find exact analytic results for the projected fluctuations.

PACS. 82.70.Dd Colloids 63.22.-mPhonons or vibrational states in low-dimensional structures and nanoscale materials 63.20.ddLattice dynamics - Measurements

1 Introduction

In a recent paper [1] we simulated a large ensemble of hard spheres packed in a face-centered cubic crystal in order to study the fluctuations within a slice of the sample. This work was motivated by the interpretation of the elastic properties found in experiments of colloidal crystals [2,3,4,5,6,7]. In particular we showed how to extract information on the three-dimensional elastic constants from the anomalous dispersion relationship that is observed within a single slice. While we managed to perform an exact analytic calculation for isotropic elastic media many experiments are performed on crystals, rather than amorphous isotropic solids. The question then arises as to how to best treat the anisotropy. We proposed using an averaging procedure such as that of Fedorov [8,9] and for the sample that we simulated the results were remarkably good: Simulation and theory agreed to within a few percent. However, many months of simulation are required to study a single sample and it is difficult to perform a systematic study of the effect of anisotropy on the projected properties.

In this paper we study the projected fluctuations within linear elasticity, rather than by molecular dynamics simulation. By formulating cubic elastic properties on a discrete grid we are able to evaluate the anisotropic Green function within a projection plane using fast Fourier transforms. This procedure allows us to study how well our analytic approximation reproduces the exact projected properties as a function of the plane orientation as well as of the three elastic constants characterizing the full cubic system.

2 Cubic Elasticity

Let us now consider a three-dimensional cubic crystal of atoms, indexed by i, deformed by the displacement vector u_i. We write the elastic energy as a quadratic form in the spatial derivatives u_{ij} of this vector. This quadratic form, which respects the symmetry of the crystal, can be expressed with the help of the Christoffel matrix [10]

$$D_{ik}(\mathbf{k}) = \Big[\lambda\delta_{ij}\delta_{kl} + \mu(\delta_{ik}\delta_{jl} + \delta_{il}\delta_{jk}) + \nu S_{ijkl}\Big] k_j k_l, \quad (1)$$

with a reciprocal vector $\mathbf{k}$, Lamé constants λ, μ and anisotropy ν. The tensor $S = \sum_{p=1}^{3} \mathbf{e}^{(p)}\mathbf{e}^{(p)}\mathbf{e}^{(p)}\mathbf{e}^{(p)}$, with $\mathbf{e}^p$ unit vectors parallel to the cubic axes of the crystal. Summation over indices occurring twice is assumed. In a colloidal crystal, being under external pressure P, the constants are modified by non-linear interactions [10]. The above constants are then related to the elastic constants used in Voigt notation,

$$\begin{aligned} C_{11} - P &= \lambda + 2\mu + \nu \\ C_{44} - P &= \mu \\ C_{12} + P &= \lambda. \end{aligned}$$

The Green function of the static elastic problem is then the inverse of the Christoffel matrix,

$$D_{ij}(\mathbf{k})G_{jk}(\mathbf{k}) = \delta_{ij}. \quad (2)$$

One expresses the free energy in terms of the displacement field

$$F[\hat{\mathbf{u}}] = \frac{1}{2}\sum_{\mathbf{k}} \hat{u}_i(\mathbf{k})D_{ij}(\mathbf{k})\hat{u}_j(-\mathbf{k}). \quad (3)$$

For each wavevector $\mathbf{k}$, D is a three-by-three matrix with eigenvalues $d_i(\mathbf{k})$ where the subscript i indicates a polarization state. Following a convention usual in the literature [11,3,7], we define the auxiliary variable $\omega_i^2(\mathbf{k}) = d_i(\mathbf{k})$.

In our previous work we showed that it was useful to perform an angular average of the elastic constants in order to generate the "best" isotropic approximation to the

elastic properties [8,9]. This average gives the effective Lamé constants

$$\tilde{\lambda} = \lambda + \frac{\nu}{5} \quad \text{and} \quad \tilde{\mu} = \mu + \frac{\nu}{5}. \tag{4}$$

On observing a slice of the three-dimensional solid under a confocal microscope one can then show that the effective dispersion described by an anomalous relation where $\omega \sim q^{1/2}$, for small $\mathbf{q}$ [1]. Here $\mathbf{q}$ is the two-dimensional wavevector, and is to be distinguished from the full three-dimensional wavevector $\mathbf{k}$. A detailed calculation gives

$$\begin{aligned} \omega_\perp^2 &= 2\tilde{\mu}\, q \quad \text{(transverse)}, \\ \omega_\parallel^2 &= \frac{4\tilde{\mu}(\tilde{\lambda}+2\tilde{\mu})}{\tilde{\lambda}+3\tilde{\mu}}\, q \quad \text{(longitudinal)}. \end{aligned} \tag{5}$$

Thus observation of the two branches of the projected dispersion curve gives information on the averaged Lamé moduli. It is interesting to note that even in the incompressible limit of rubber elasticity where $\mu/\lambda \to 0$ the effective projected frequencies remain finite. Apparent compression in the two-dimensional plane remains easy. In this limit we find that $\omega_\perp^2/\omega_\parallel^2 = 1/2$.

3 Discretization

Rather than performing a molecular dynamics simulation of hard spheres, we here use only methods from linear algebra to numerically project and characterize fluctuations from an elastic solid. The disadvantage is that all nonlinearities in the true physical system are neglected. The advantage is that very efficient methods are available that generate useful data in just a few minutes of calculation. One is also able to systematically vary the parameters of the model in order to study their influence on the projected fluctuations.

We use a finite difference discretization of Eq. (1), taking the mesh size as unity and embedding the elastic medium in a cubic box of dimensions L. For any wavevector $\mathbf{k}$ we define the components of a vector $\mathbf{v}$ as

$$v_j = (1 - e^{ik_j}). \tag{6}$$

The finite different discretization corresponding to Eq. (1) is then

$$D = \mu\, z(\mathbf{k})\, \mathbf{I} + (\lambda+\mu)(\mathbf{v} \otimes \mathbf{v}^*) + \nu\ \mathrm{diag}(v_i v_i^*), \tag{7}$$

with $z(\mathbf{k}) = \mathrm{tr}(\mathbf{v}\otimes\mathbf{v}^*) = \sum_i (2-2\cos k_i)$ and where "diag" constructs a three-by-three matrix with the given components on the diagonal. $\mathbf{I}$ is the three-dimensional unit matrix, and $\otimes$ denotes the exterior product of two vectors. The matrix D is complex Hermitian. One sees that the small-wavevector expansions of Eq. (7) is indeed given by the Christoffel matrix. The exact analytic form makes the dispersion relation periodic within the first Brillouin zone of the discretizing mesh. Note this form of the discretization suffices to study cuts in the plane $(1,0,0)$. Other cuts are found by rotating the crystal with respect to the cubic cell, modifying the contribution in ν. This is easily performed by updating the tensor S using rotation matrices parameterized with Euler angles.

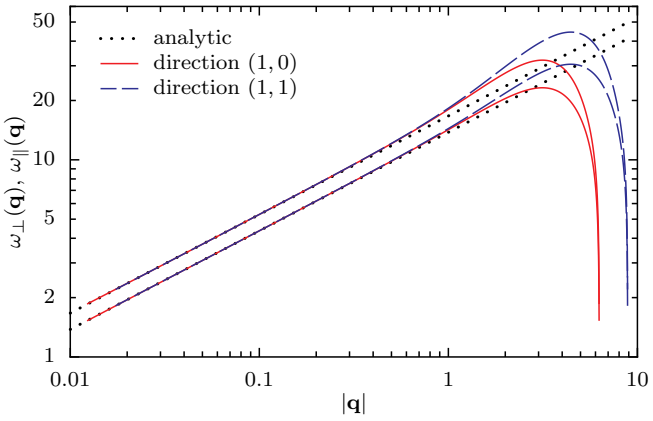

Figure 1. Longitudinal and transverse fluctuations of an isotropic system projected to the two-dimensional plane $(1,0,0)$. The result is compared to the long-wavelength limit (dotted line) predicted in Eq. (5). $L = 512$, $\lambda = 70$, $\mu = 95$, $\nu = 0$.

We evaluate $D(\mathbf{k})$ for wavevectors $k_i = 2\pi n_i/L$. We numerically invert the three-by-three matrix $D(\mathbf{k})$ for each value of $\mathbf{k}$ and then use the fast Fourier transform to evaluate the components of the real space Green function on a cubic grid. We then evaluate the Green functions on a slice and use two-dimensional fast Fourier transforms to obtain the effective dispersion relation for a projected wavevector $\mathbf{q}$. Such a dispersion relation is shown in Fig. 1 for the isotropic case $\nu = 0$, where we compare with the continuum expressions Eq. (5). As expected, we see agreement between theory and simulation. We use values of μ and λ comparable to those found in our previous molecular dynamics simulations. The anisotropy ν will be varied over a wide range of values in the figures below. We use units such that the energy scale is $k_B T$.

We now show how to calculate the full dispersion curve corresponding to the present discretization, using a alternative calculational route than that proposed in our original paper.

3.1 Projection for $\nu = 0$

In our previous work we gave a treatment of the projection which required calculation of the explicit form of the real-space Green function. We show here that a different method allows one to calculate the projection for $\nu = 0$, and we apply this method to the discretized Eq. (7), generating the analytic expression for the full curves of Fig. 1. We firstly calculate the inverse of Eq. (7)

$$G(\mathbf{k}) = \frac{1}{\mu z(\mathbf{k})}\left(\mathbf{I} - \frac{\lambda+\mu}{\lambda+2\mu}\frac{\mathbf{v}\otimes\mathbf{v}^*}{z(\mathbf{k})}\right). \tag{8}$$

We now formally calculate the real-space Green function by Fourier transformation, and back transform the pro-

jected correlations. Elementary calculations show that

$$G_2(\mathbf{q}) = \sum_{k_z} G(q_x, q_y, k_z) \to \frac{1}{2\pi}\int_{-\pi}^{\pi} dk_z G(\mathbf{q}, k_z), \quad (9)$$

where G_2 describes the correlations projected on the confocal plane $z = 0$.

The integral is calculated by noting that

$$\frac{1}{2\pi}\int_{-\pi}^{\pi} \frac{1}{A - 2\cos k_z} dk_z = \frac{1}{(A^2-4)^{1/2}},$$
$$\frac{1}{2\pi}\int_{-\pi}^{\pi} \frac{1}{(A - 2\cos k_z)^2} dk_z = \frac{A}{(A^2-4)^{3/2}}.$$

Within the plane we consider without loss of generality the choice $\mathbf{q} = (q, 0)$, then $A = 4 - 2\cos q$. The dispersion relations are then

$$\frac{1}{\omega_\perp^2} = \frac{1}{\mu}\frac{1}{\left[(4-2\cos q)^2 - 4\right]^{1/2}}, \quad (10)$$
$$\frac{1}{\omega_\parallel^2} = \frac{1}{\omega_\perp^2} - \frac{1}{\mu}\frac{\lambda+\mu}{\lambda+2\mu}\left(\frac{(4-2\cos q)(2-2\cos q)}{\left[(4-2\cos q)^2-4\right]^{3/2}}\right).$$

When one expands Eq. (10) about $q = 0$ one finds exactly Eq. (5). It should be noted that all higher order corrections in the expansion of Eq. (10) are non-universal, and thus change on using different discretizations of the continuum equations. However these equations are useful in calibrating the convergence of the numerical code that we developed for this paper.

4 Three-dimensional structure of fluctuations

In this section we discuss the three-dimensional nature of the fluctuation field induced in the presence of a fluctuation in a surface. In particular we wish to argue that the use of periodic boundary conditions does not lead to strong artifacts in the amplitudes of the measured waves, at the same time we are able to estimate the decay of boundary perturbations to a sample on fluctuations within a sample. Very similar arguments are regularly used in electrostatics [12,13]. Let use firstly summarize the situation for solutions of the Laplace equation where the algebra is particularly simple.

Consider a periodic box of lateral dimensions L and height L_z. Let there be charges on the plane $z = 0$ modulated with wavevector k_x. Away from the plane, in the absence of sources, the potential is given by a solution to the equation $\nabla^2\phi = 0$. If the solution is periodic in the $x-y$ plane then the solution must decay exponentially in the z direction so that

$$\phi = \phi_k \exp(ikx - k|z|). \quad (11)$$

The slowest decaying wave in the z direction has $k = 2\pi/L$, thus successive images in the box have an asymptotic interaction [12] that varies as $\sim e^{-2\pi L_z/L}$. Already in a cubic box, for which $L_z = L$ the image interaction via this component of the density is strongly suppressed. Higher order waves have even weaker interactions.

We now return to the problem of an isotropic elastic solid. If we observe a sinusoidal perturbation on the plane $z = 0$ we can find the minimum energy fluctuation consistent with this observation by examining the solution of the equation

$$(1-2\sigma)\nabla^2\mathbf{u} + \operatorname{grad}\operatorname{div}\mathbf{u} = 0 \quad (12)$$

away from the plane $z = 0$, where σ is the Poisson ratio of the material. We look for solutions of the form

$$\mathbf{u} = e^{ikx}(u(z), 0, w(z)) \quad (13)$$

and find

$$(1-2\sigma)(-k^2+\gamma^2)u - k^2u + ik\gamma w = 0,$$
$$(1-2\sigma)(-k^2+\gamma^2)w + \gamma^2 w + ik\gamma u = 0,$$

where γ is the Laplace transform of the fields in the z direction. Solution are found when the determinant of coefficients is zero which gives

$$k^2 = \gamma^2,$$

implying a result very similar to that in electrostatics: There is a decay of interactions on a scale which is determined by the wavelength of the observed mode, independent of the Poisson ratio. There is also a simple phase relationship between the horizontal and vertical components of the fluctuations:

$$u \pm iw = 0$$

From this calculation we understand that we should only observe samples far from any external walls. Fluctuations of wavelength ℓ observed within a plane decay over a distance $\ell/2\pi$ and will be perturbed by external surfaces which are too close. This result allows us to find a simple physical interpretation of the anomalous dispersion relation: Imposition of a fluctuation of wavelength ℓ leads to an energy density $(u/\ell)^2$. This excites a total volume of the sample which varies as $L^2\ell$, giving a scaling in the total elastic energy $1/\ell \sim |q|$.

We now study the variation of the elastic properties as a function of the cubic anisotropy ν, and compare the results with the averaging approximation.

5 Numerical Results

We implemented the Fourier and matrix manipulation using an Octave/Matlab script; the language was chosen for its facilities for the manipulation of fast Fourier transforms and matrix algebra. We projected the fluctuations onto different planes of the crystal and study the effective dispersion relations, Fig. 2. For the cut of the crystal in the plane $(1, 0, 0)$ we plot the effective dispersion relations in two directions in the plane, $(1, 0)$ and $(1, 1)$. The averaging

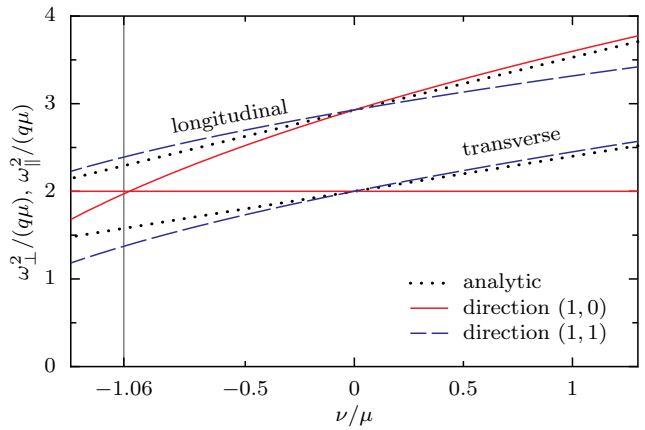

Figure 2. Evolution of amplitudes as a function of ν in a cut perpendicular to $(1,0,0)$. Previous theory in dotted line, Eq. (5). The theoretical curves are intermediate between the two numerically generated curves. The curve in the direction $(1,0)$ displays the exceptional features to be independent of ν. All lines intersect at $\nu = 0$ since the system becomes isotropic. $L = 512$. $\lambda/\mu = 0.73$.

approximation, while not wholly inaccurate, does not account for a number of qualitative features of the measured dispersion curves. In particular, the measured transverse stiffness in the direction $(1,1)$ is *independent* of ν while the longitudinal mode varies strongly with the anisotropy. This gives rise to level crossing for large negative values of ν.

The situation in the plane $(1,1,0)$, Fig. 3, is somewhat closer to the approximate analytic form of the dispersion curves. Here again the dispersion is anisotropic within the plane. Clearly this is impossible to describe with spherically averaged elastic constants.

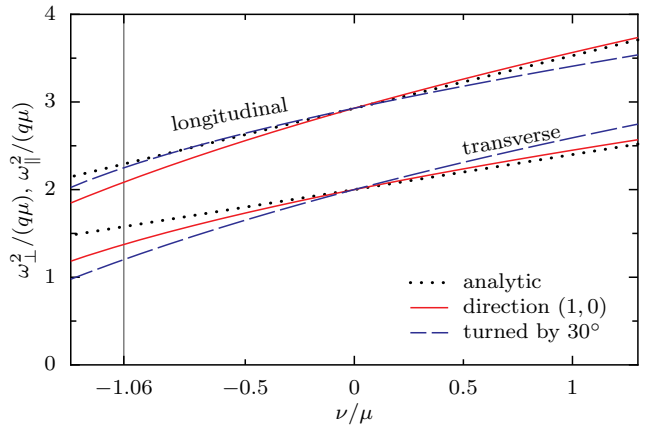

Figure 3. Evolution of amplitudes as a function of ν in a cut perpendicular to $(1,1,0)$. $L = 512$. $\lambda/\mu = 0.73$.

For the plane $(1,1,1)$, Fig. 4 we see that the averaging procedure works particularly well and that the dispersion relations are isotropic. This is the curve which is the most useful experimentally, because the samples naturally grow from flat surfaces aligned in this orientation.

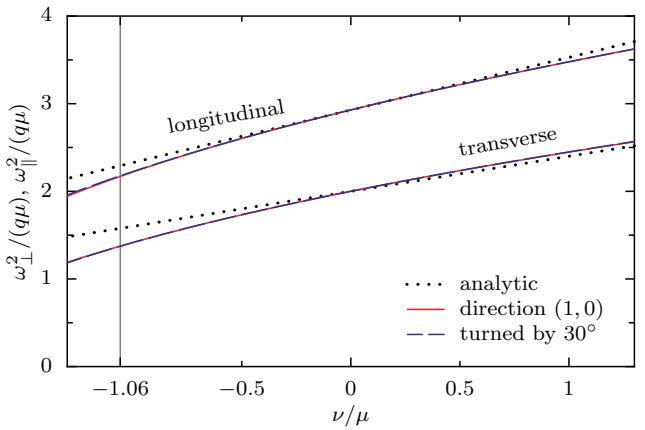

Figure 4. Evolution of amplitudes as a function of ν in a cut perpendicular to $(1,1,1)$. The dispersion curve is isotropic in the plane. $L = 512$. $\lambda/\mu = 0.73$.

The vertical gray lines in Figs. 2–4 at $\nu/\mu = -1.06$ represent the anisotropy found in the full molecular-dynamics simulation. Also the ratio λ/μ has been chosen to fit to the simulation. Comparing the published data [1] with Fig. 4, we notice that the full simulation curves are displaced with respect to the data produced by Fourier analysis. Both are slightly displaced with respect to the isotropic average, but with different signs. We interpreted this shift as being due to non-linearities in the full system and estimated it to about 3%. A new estimate based on the numerical method described in this paper is larger, about 9% and 15%.

5.1 Analytic projection on $(1,0,0)$

Using the method of Sec. 3, it is easy to write a formal solution for the projected properties for arbitrary ν. In the limit of small $\mathbf{q}$ one finds as integrand the ratio of two polynomials of orders four and six in the vector (q_x, q_y, k_z), see also [14]. In principle by factorizing the denominator (which is of order six) one has the full analytic solution to the problem. In practice this requires the roots of high order equations and leads to clumsy and opaque expressions. There is, however, one case which is particularly easy to understand, namely the independence of the transverse mode in Fig. 3 on ν. This is a simple consequence of the Sherman-Morrison identity: The Christoffel matrix on the plane $(1,0,0)$ can be written as a diagonal matrix plus a rank one update:

$$\begin{aligned} D &= B + (\lambda+\mu)(\mathbf{k}\otimes\mathbf{k}), \\ \text{with}\quad B &= \mathrm{diag}(\mu k^2 + \nu k_i^2). \end{aligned}$$

The inverse of this matrix is then

$$G = B^{-1} - \frac{(\lambda+\mu)(B^{-1}\mathbf{k})\otimes(B^{-1}\mathbf{k})}{1+(\lambda+\mu)\mathbf{k}B^{-1}\mathbf{k}}. \qquad (14)$$

If $\mathbf{q} = (1,0)$, then it is clear that $G_{xy}(1,0,k_z) = 0$ and the only contribution to the projected transverse spectrum

comes from $G_{yy}(1,0,k_z)$ which is trivially independent of ν.

The longitudinal contribution can also be found from the Sherman-Morrison formula, we find the integral:

$$\frac{\mu q}{\omega_\parallel^2} = \int_{-\pi}^{\pi} \frac{dk}{2\pi} \frac{1}{1+\nu/\mu+k^2} \times \left[1 - \frac{1+k^2+k^2\nu/\mu}{\frac{(1+\nu/\mu+k^2)(1+k^2+k^2\nu/\mu)}{1+\lambda/\mu} + 1 + 2(1+\nu/\mu)k^2 + k^4}\right]$$

This can be integrated by finding the roots of the denominator, and expanding using partial fractions, the result is however too complicated to be illuminating.

5.2 Simulation data

On seeing the surprising nature of the dispersion in Fig. 2 where the longitudinal and transverse modes becomes almost degenerate at large negative values of the anisotropy, around $\nu \sim -\mu$, we performed an analysis based on our molecular dynamics simulation, Fig. 5. There, the anisotropy was also strong, $\nu = -1.06\mu$. We find that indeed our numerical data displays very similar features, confirming the useful nature of the Fourier based code for exploring the properties of the elastic behavior of hard sphere systems. The longitudinal and transverse dispersion relations are almost degenerate over all wavevectors in the direction $(1,0)$. We do not have any simple explanation for this result.

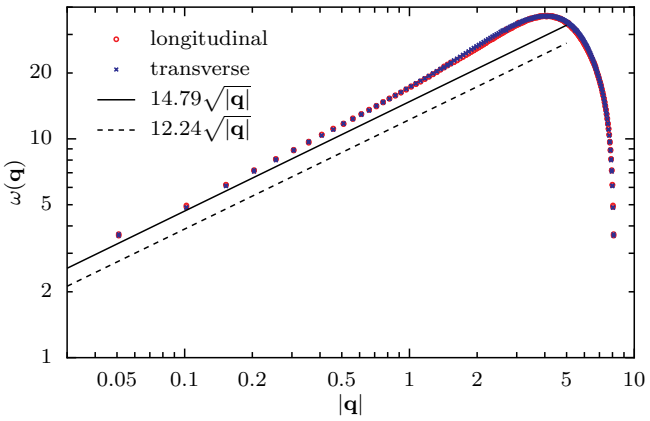

Figure 5. Effective dispersion relations for the plane $(1,0,0)$ in the direction $(1,0)$. Dataset of [1]. The longitudinal and transverse branches are almost degenerate at the large negative cubic anisotropy.

6 Density of states

In the interpretation of the density of states of disordered material one often compares with the Debye theory of elasticity. This allows one to establish an expectation for the low-frequency mode structure, and then to determine whether the disorder has given rise to a deficit or excess in the density of states. As noted in [15] a dispersion relation such as Eq. (5) leads to modifications in the Debye spectrum, which is normally given as $\rho(\omega) \sim \omega^{d-1}$ for a d-dimensional elastic solid. If we use instead the dispersion relations in Eq. (5) and define $\omega_\parallel^2 = a_\parallel q$ and $\omega_\perp^2 = a_\perp q$ we find that the density of states, expressed in terms of the variable ω is given by

$$\rho(\omega) = \frac{1}{\pi}\Big(\frac{1}{a_\parallel^2} + \frac{1}{a_\perp^2}\Big)\omega^3, \qquad (15)$$

which corresponds to neither the projected, nor the embedding dimension of the slice. Figure 6 shows the density of states of a cut of our molecular dynamics crystal. The top panel displays the binned density of states on a linear scale. In order to avoid artifacts of binning we also plot the integrated density of states in the bottom panel and find that there is a good fit to a law in ω^4 for $\omega < 8$. Some of the experimental literature plots two-dimensional slices normalized by the Debye density of states for a three-dimensional crystal [5]. We have also plotted this form in the top panel of Fig. 7. We see, rather surprisingly, a region between the local frequency behavior in ω^3 and the first peak where the normalized data seems relatively

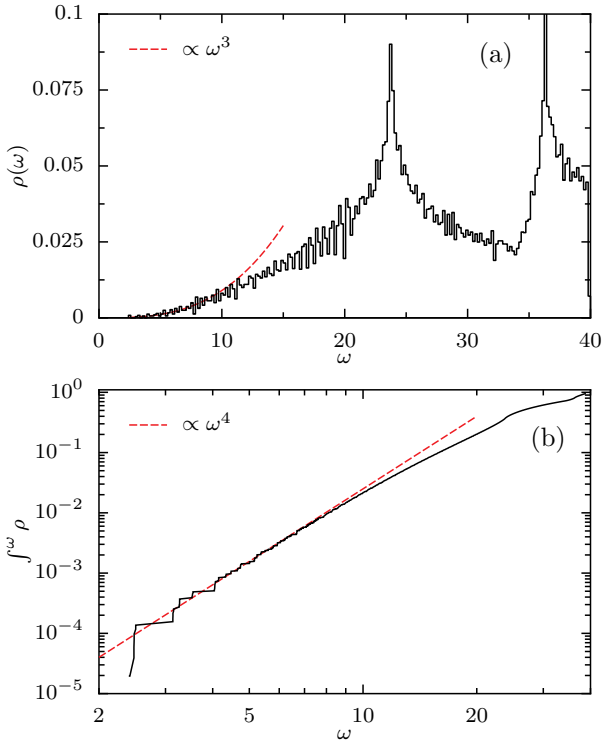

Figure 6. Density of states measured on the $(1,1,1)$ cut, data from the molecular dynamics simulation [1]. (a) Note the prominent van Hove singularities corresponding to the longitudinal and transverse projected modes. Panel (b) plots the integrated density of states on a log-log scale, compared with the theoretical form ω^4.

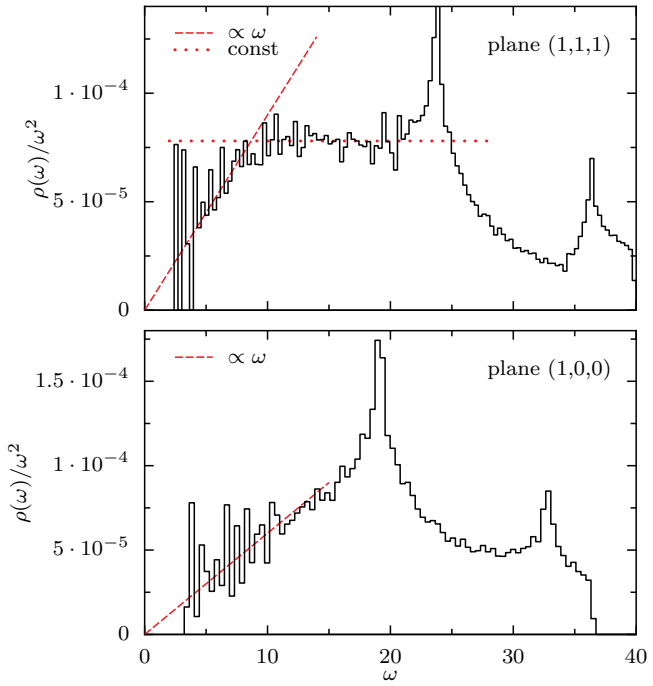

Figure 7. Density of states divided by ω^2, projected on two different planes. The resulting curves depend on the projection plane: In the case $(1,1,1)$ the expect regime in $\rho \sim \omega^3$ is seen for $\omega < 10$; a plateau is observed for $10 < \omega < 20$. The form $\rho \sim \omega^3$ fits over a larger range of ω for the case $(1,0,0)$.

constant. This seems, however, to be a simple cross-over occurring over a modest range of frequencies. If we project on a different plane, $(1,0,0)$ in the bottom panel of Fig. 7, no plateau is visible.

7 Conclusions

We have introduced a Fourier based method which can efficiently generate the Green function in anisotropic elastic media. It allows one to rapidly perform detail studies of the evolution of correlations and fluctuations in projected geometries, such as those used in several recent experiments. We have studied the effective dispersion relations of a colloidal crystal projected to the plane $(1,0,0)$ and shown that the near degeneracy of the dispersion curves in the direction $(1,0)$ is due to the large negative cubic anisotropy. Surprisingly long wavelengths are needed to see continuum limit in the density of states. Studies on certain cuts lead to an intermediate regime for the density of states.

Code written in Octave/Matlab is available as supplementary material to the paper to perform the Fourier based evaluation of Green functions, together with the projection to two dimensions.

References

1. C.A. Lemarchand, A.C. Maggs, M. Schindler, ArXiv e-prints (2011), 1103.2937
2. K. Zahn, A. Wille, G. Maret, S. Sengupta, P. Nielaba, Phys. Rev. Lett. **90**(15), 155506 (2003)
3. P. Keim, G. Maret, U. Herz, H.H. von Grünberg, Phys. Rev. Lett. **92**(21), 215504 (2004), http://prl.aps.org/abstract/PRL/v92/i21/e215504
4. K. Chen, W.G. Ellenbroek, Z. Zhang, D.T.N. Chen, P.J. Yunker, S. Henkes, C. Brito, O. Dauchot, W. van Saarloos, A.J. Liu et al., Phys. Rev. Lett. **105**(2), 025501 (2010)
5. D. Kaya, N.L. Green, C.E. Maloney, M.F. Islam, Science **329**(5992), 656 (2010)
6. A. Ghosh, R. Mari, V. Chikkadi, P. Schall, J. Kurchan, D. Bonn, Soft Matter **6**(13), 3082 (2010), http://dx.doi.org/10.1039/c0sm00265h
7. A. Ghosh, V.K. Chikkadi, P. Schall, J. Kurchan, D. Bonn, Phys. Rev. Lett. **104**(24), 248305 (2010)
8. A.N. Norris, J. Acoust. Soc. Am. **119**(4), 2114 (2006)
9. A.F.I. Fedorov, *Theory of Elastic Waves in Crystals* (Plenum Press, New York, 1968)
10. D.C. Wallace, *Thermoelastic Theory of Stressed Crystals and Higher-Order Elastic Constants* (Academic Press, New York and London, 1970), Vol. 25, pp. 301–404
11. Z. Cheng, J. Zhu, W.B. Russel, P.M. Chaikin, Phys. Rev. Lett. **85**(7), 1460 (2000)
12. I.C. Yeh, M.L. Berkowitz, J. Chem. Phys. **111**(7), 3155 (1999)
13. L. Levrel, A.C. Maggs, The Journal of Chemical Physics **128**(21), 214103 (8) (2008), http://link.aip.org/link/?JCP/128/214103/1
14. A. Morawiec, Phys. Stat. Sol (b) **184**(2), 313 (1994)
15. A. Ghosh, R. Mari, V.K. Chikkkadi, P. Schall, A.C. Maggs, D. Bonn, ArXiv e-prints (2011), 1102.4271